variations in the butene ion distributions with energy (Table VI) by assuming that the high energy excited state of the parent ion (whose decomposition is exemplified by reactions 36, 37, and 38) leads to the excited $C_4H_8^+$ species which undergoes reactions 39 and 40. Thus, we see that the formation of the 2-butene and isobutylene ions are especially important in the krypton-sensitized radiolysis. On the other hand, in the xenon-sensitized radiolysis, the long-lived, low energy state of the $C_6H_{12}^+$ ion yields mainly the 1-$C_4H_8^+$ ion by a concerted unimolecular mechanism even though the heat of formation of the 1-butene ion is greater than that of the 2-butene ion.

In view of the energy dependence on the distribution of the butene ion isomers, it may be anticipated that the relative abundances will also be dependent on the pressure of the system. In accordance with the above interpretation, photoionization experiments which will be reported at a later date[11] show that the yields of both the isobutylene ion and 2-butene ion diminish relative to the 1-butene ion yield with an increase in pressure of either the cycloalkane or a rare gas additive.

Acknowledgment. The authors have included in Tables IV and V some hitherto unpublished results of several experiments performed in the course of other investigations by Drs. J. Herman, K. Herman, and R. D. Doepker.

---

(11) P. Ausloos, submitted for publication.

Analysis of the Ion–Molecule Reactions in Hydrogen–Methane Mixtures Using Ion Cyclotron Resonance[1]

Michael T. Bowers and Daniel D. Elleman

Contribution from the Department of Chemistry, University of California, Santa Barbara, California 93106, and the Jet Propulsion Laboratory, California Institute of Technology, Pasadena, California 91103.

Received July 31, 1969

Abstract: The kinetics and energetics of the principal ion–molecule reactions in hydrogen–methane mixtures are reported. The emphasis is on the reactions of H_3^+ with neutral methane. The pressure dependence of the $CD_4H^+/\Sigma C(H,D)_3^+$ ratio as a function of H_2 pressure in a CD_4–H_2 mixture is presented. In order to explain the details of the pressure dependence, reactions of both excited $[H_3^+]^*$ and collisionally deactivated H_3^+ with CD_4 are postulated. $[H_3^+]^*$ forms CD_3^+ and CD_2H^+ primarily *via* a direct mechanism, while H_3^+ first forms $[CD_4H^+]^*$, which is subsequently collisionally stabilized or decomposes to CD_3^+ or CD_2H^+. Pulsed-ion-ejection double resonance studies support this interpretation and indicate both hydride ion abstraction and some sort of displacement mechanism are simultaneously at play in the direct formation of CD_3^+ and CD_2H^+. The lifetime of the $[CD_4H^+]$ ion was determined to be approximately 2×10^{-4} sec, nearly two orders of magnitude longer than previously estimated by Aquilanti and Volpi.

Ion cyclotron resonance (icr) spectroscopy is rapidly becoming established as a prime tool for studying a wide variety of gas phase ion–molecule processes.[2–5] Of particular interest in these laboratories is the use of icr to determine quantitative kinetic data[5–8] and detailed mechanistic information[6–8] on simple systems of atmospheric importance. Investigations to date have dealt with H_2,[6] $H_2 + N_2$ mixtures,[7,8] and $H_2 + Ar$ mixtures.[8] In this report these studies are extended to include the various ion–molecule reactions in H_2–CH_4 mixtures, a system of considerable importance in the study of the Jovian atmosphere,[9] and possibly crucial to the understanding of the evolution of the earth's primitive reducing atmosphere.

The hydrogen–methane system has been studied by several authors,[10–12] the most recent work being by Aquilanti and Volpi[12] using a high-pressure mass spectrometer with a tritium ionization source. The experiments of Aquilanti and Volpi[12] were restricted to measuring the rate of reaction of H_3^+ with CH_4 and to observing the resulting CH_5^+/CH_3^+ ratio as a function of H_2 pressure. The ratio data of this labotatory agree qualitatively with theirs at high H_2 partial pressures. At lower pressures, however, our data conclusively show curvature and a nonzero intercept while they[12] assume the linear decrease in CH_5^+/CH_3^+ continues to a value of zero at zero H_2 pressure. Aquilanti and Volpi[12] interpret their ratio data by assuming collisional stabilization of excited $[CH_5^+]^*$ by H_2. Our additional

---

[1] Supported in part by Contract No. NAS7-100 extended to the Jet Propulsion Laboratory by the National Aeronautics and Space Administration.

[2] J. L. Beauchamp, L. R. Anders, and J. D. Baldeschwieler, *J. Amer. Chem. Soc.*, **89**, 4569 (1967).

[3] J. D. Baldeschwieler, *Science*, **159**, 263 (1968).

[4] (a) J. L. Beauchamp, *J. Chem. Phys.*, **46**, 1231 (1967); (b) J. L. Beauchamp and S. E. Buttrill, *ibid.*, **48**, 1783 (1968).

[5] M. T. Bowers, D. D. Elleman, and J. L. Beauchamp, *J. Phys. Chem.*, **72**, 3599 (1968).

[6] M. T. Bowers, D. D. Elleman, and J. King, Jr., *J. Chem. Phys.*, **50**, 4787 (1969).

[7] M. T. Bowers, D. D. Elleman, and J. King, Jr., *ibid.*, **50**, 1840 (1969).

[8] M. T. Bowers and D. D. Elleman, *ibid.*, **51**, 4606 (1969).

[9] G. P. Kuiper, "The Atmospheres of the Earth and Planets," University of Chicago Press, Chicago, Ill., 1952, p 306.

[10] S. Wexler, *J. Amer. Chem. Soc.*, **85**, 272 (1963).

[11] M. S. B. Munson, J. L. Franklin, and F. H. Field, *ibid.*, **85**, 3584 (1963).

[12] V. Aquilanti and G. G. Volpi, *J. Chem. Phys.*, **44**, 2307 (1966).

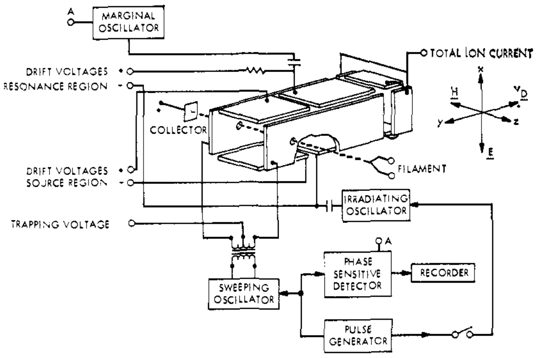

Figure 1. Schematic view of the icr cell showing the various irradiation possibilities.

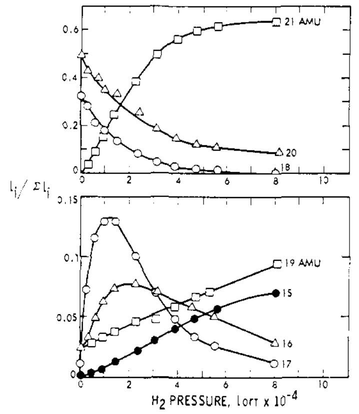

Figure 2. Plot of relative intensities of molecules with one carbon *vs.* H_2 partial pressure for H_2–CD_4 mixtures. CD_4 was at a constant pressure of 6×10^{-6} Torr, electron energy was 40 eV, and electron current 1×10^{-8} A. Residence time in the cell, $\tau \cong 7 \times 10^{-4}$ sec.

low pressure data indicate that a much more complicated reaction mechanism is needed. Specifically, there is evidence for including reactions of two kinds of H_3^+ ion with CH_4; an excited $[H_3^+]^*$ ion and a collisionally deactivated H_3^+ ion. Details are given in the discussion section.

During the course of this work, Leventhal and Friedman[13] published a paper on energy transfer from excited $[H_3^+]^*$ ions. They reacted $[H_3^+]^*$ with CH_4 in a tandem mass spectrometer and plotted the resulting CH_5^+/CH_3^+ ratio as a function of H_2 pressure. Their results qualitatively agreed with our results at low H_2 pressures where a nonzero intercept for CH_5^+/CH_3^+ was found. Quantitative comparison with their work[13] is difficult, however, as they were working with H_3^+ ions with at least 3.5 eV of translational energy. Hence, relatively more decomposition product (CH_3^+) was found at all H_2 pressures.

In the second section, the experimental details are given. In the third part, the experimental results are given and discussed. Specific experimental techniques include pressure dependence plots, ion-ejection experiments, and double resonance experiments. Considerations of all three techniques lead to a complete picture of the detailed reaction scheme for H_2–CH_4 mixtures.

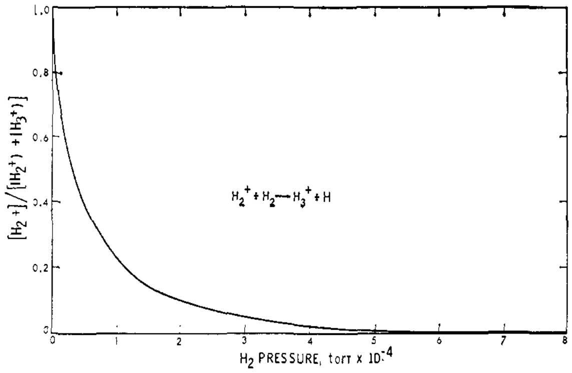

Figure 3. Relative abundance of $[H_2^+]$ *vs.* $[H_3^+]$ as a function of H_2 pressure. Residence time in the cell, $\tau \cong 5 \times 10^{-4}$ sec.

Experimental Section

The icr spectrometer used for these studies is of conventional design and has been discussed in detail previously.[5-8] A schematic diagram is given in Figure 1, showing the icr cell and the arrangement of the various irradiation schemes.

The pressure was measured using a General Electric ion gauge circuit standardized for N_2. Corrections were made for differences between the ionization cross section of the sample gases and N_2. A further correction was made by calibrating the pressure against the reaction[14]

$$CH_4^+ + CH_4 \longrightarrow CH_5^+ + CH_3$$

In order to accurately determine the partial pressure of H_2 in the CH_4–H_2 mixtures, a dual inlet system was employed. CH_4 was usually introduced through a fixed leak valve bringing the pressure to nominally 3×10^{-6} Torr. H_2 was then bled in through a variable leak valve controlled by a Granville-Phillips automatic pressure controller. In calculating the partial pressure of H_2 it was assumed that the collection efficiency of the ion gauge was the same for all ions.

The H_2 and D_2 gases used were Matheson prepurified grade. The CH_4 was Matheson research grade, the CD_4 and CH_3D Merck Sharp and Dohme. Small impurities of CD_3H and CH_4 were present in CD_4 and CH_3D, respectively. Finally, a small amount of H_2O impurity persisted at higher pressures despite repeated bakeout of the icr cell and sample inlet line. However, the H_2O impurity did not introduce a serious ambiguity in the interpretation of the experimental results.

Results

A. Pressure Dependence. In Figure 2, the dependence of intensities of the molecules with one carbon atom in CD_4–H_2 mixtures are given as a function of the H_2 pressure.

A similar plot is given in Figure 3 for the ratio of $[H_2^+]/([H_2^+] + [H_3^+])$ over the pressure range of interest. H_3^+ is formed by the reaction

$$H_2^+ + H_2 \longrightarrow [H_3^+]^* + H \qquad (1)$$

where $[H_3^+]^*$ has of the order of 2-eV internal energy.[15] The internal energy of $[H_3^+]^*$ is rapidly moderated by subsequent collisions with H_2.

$$[H_3]^* + H_2 \longrightarrow H_2^* + H_3^+ \qquad (2)$$

Leventhal and Friedman[13] have shown that as few as one collision may completely moderate the $[H_3^+]^*$ ion. At the higher H_2 partial pressures studied here, a large majority of the $[H_3^+]^*$ is thus moderated, while at lower H_2 partial pressure, the reaction of $[H_3^+]^*$ must be considered. The final vibrational state of the H_3^+ ion

---

(13) J. J. Leventhal and L. Friedman, *J. Chem. Phys.*, **50**, 2928 (1969).

(14) S. K. Gupta, E. G. Jones, A. G. Harrison, and J. J. Myher, *Can. J. Chem.*, **45**, 3107 (1967)

(15) J. J. Leventhal and L. Friedman, *J. Chem. Phys.*, **49**, 1975 (1968).

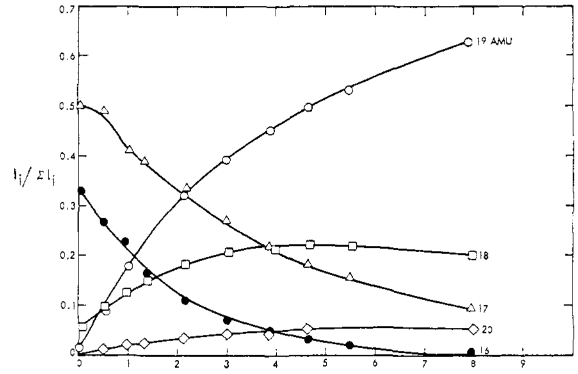

Figure 4. Plot of relative intensities of molecules with one carbon atom as a function of D_2 pressure in a D_2–CH_3D mixture. Same conditions as Figure 2.

generated by the deactivation process of reaction is not known. It probably is not the ground vibrational state unless accidental resonances occur between the vibrational levels of H_3^+ and H_2. This question is currently undergoing further study in these laboratories.

Returning to Figure 2, the major single carbon product is protonated CD_4 formed by the reaction

$$H_3^+ + CD_4 \longrightarrow CD_4H^+ + H_2 \qquad (3)$$

In addition to the major CD_4H^+ product, minor products are detected at 15, 16, 17, and 19 amu. The mass 17, 16, and 15 products correspond to CD_2H^+, CDH_2^+, and CH_3^+ formed principally *via* the chain reaction sequence

$$CD_3^+ + H_2 \longrightarrow CD_2H^+ + HD \qquad (4)$$

$$CD_2H^+ + H_2 \longrightarrow CDH_2^+ + HD \qquad (5)$$

$$CDH_2^+ + H_2 \longrightarrow CH_3^+ + HD \qquad (6)$$

This reaction sequence was initially suggested by the work of Wexler,[10] more conclusively demonstrated by Munson, Field, and Franklin,[11] and convincingly reaffirmed by our pressure data and double resonance results. In the following section it will be shown that CD_3^+ and CD_2H^+ are also formed from the reactions of $[H_3^+]^*$ and CD_4.

The mass 19 peak increases linearly in pressure over the entire pressure range studied. There are two likely possibilities.

$$CD_4^+ + H_2 \longrightarrow CD_3H^+ + HD \qquad (7)$$

$$H_3^+ + H_2O \longrightarrow H_3O^+ + H_2 \qquad (8)$$

Reaction 7 would give the proper pressure dependence and is expected to have a rate constant of approximately 1×10^{-10} cc molecule^{-1} sec^{-1}.[11] The probability that 8 contributes (at least in part) to mass 19 is enhanced by the double resonance results (discussed in the following section), which give a negative response when mass 19 is observed and mass 3 irradiated.

The two processes corresponding to 7 and 8 can be separated in the CH_3D–D_2 system. The appropriate pressure plot is given in Figure 4. The reactions of interest are

$$CH_3D^+ + D_2 \longrightarrow CH_2D_2^+ + HD \qquad (9)$$

$$D_3^+ + H_2O \longrightarrow H_2DO^+ + D_2 \qquad (10)$$

It is noted that both the mass 18 and 20 peaks increase with D_2 concentration, indicating that both processes are occurring. Considerable effort was employed to eliminate the H_2O impurity, to no avail. The remainder of the pressure dependence in Figure 4 can be explained by reactions similar to 3–7.

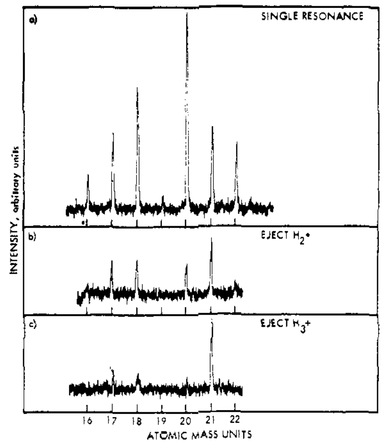

Figure 5. Pulsed-ion-ejection spectra of CD_4–H_2 mixture: partial pressures of CD_4, 7.5×10^{-6} and of H_2, 2×10^{-4} Torr, electron energy 40 eV, and electron current 1×10^{-8} A. Residence time in the cell, $\tau \cong 7 \times 10^{-4}$ sec. Part a is the single resonance spectra, part b the pulse ejected spectra of H_2^+, and part c the pulse ejected spectra of H_3^+.

B. Ion-Ejection Studies. The ion-ejection technique was recently introduced by Beauchamp and Armstrong[16] and is very useful for studying systems where reactant and product ions differ considerably in mass and concurrent reactions make direct interpretation of single resonance spectra difficult. The trapping voltage applied to the side plates of the icr cell (Figure 1) creates a potential well in which the ions oscillate parallel to the magnetic field at frequency $\omega = (4qV_T/md^2)^{1/2}$, where q is the ion charge, V_T the trapping voltage, m the ion mass, and d the cell width. Since ω is mass dependent, a particular ion can be ejected from the cell (*i.e.*, neutralized on the trapping plates) by applying an oscillating rf field to the trapping plates without disturbing the reactions of the remaining ions. The ions are ejected in time[16] $\tau_e = m\omega d/q\mathcal{E}_{rf}$ where $\mathcal{E}_{rf}$ is the electric field strength of the oscillator at frequency ω. τ_e can easily be set to be much less than the total drift time of the ions. In the standard icr experiment either the drift field or magnetic field is modulated and the output of the marginal oscillator detector fed into the phase sensitive detector. In a pulsed-ion-ejection experiment, the ejection field, $\mathcal{E}_{rf}$, is modulated, resulting in a phase detected signal characteristic of the ejected species only. This type of experiment is easily adapted to the H_2–CD_4 system.

In Figure 5, the results of such an experiment are presented. The H_3^+ ejection spectrum in Figure 5c clearly shows that essentially all of the CD_4H^+ originates from H_3^+ ions. Minor contributions of H_3^+ to the CD_3^+ and CD_2H^+ masses are also evident. The small response at mass 20 may indicate an H_3^+–CD_4 charge exchange process, but the energetics of the reaction are unfavorable.[17] The possibility that it could be due to

---

(16) J. L. Beauchamp and J. T. Armstrong, *Rev. Sci. Instrum.*, **40**, 123 (1969).

(17) The ionization potential of CD_4 is 13.19 eV (R. W. Kiser, "Introduction to Mass Spectrometry," Prentice-Hall, Inc., Englewood Cliffs, N. J., 1965, Appendix IV). The ionization potential of H_3^+ has been estimated at 10.77 eV (linear), and 8.62 eV (triangular): J. J. Leventhal

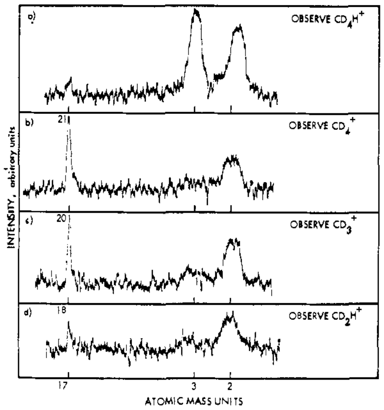

Figure 6. Frequency sweep ion-ejection spectra of CD_4–H_2 mixture: partial pressures of CD_4, 7.5×10^{-6} and of H_2, 2×10^{-4} Torr, 1×10^{-8} A electron current, and 40-eV electron energy.

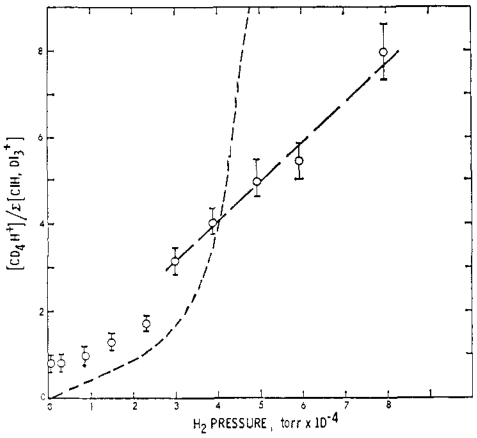

Figure 7. Plot of $[CD_4H^+]/([CD_3^+] + [CD_2H^+ + [CDH_2^+] + [CH_3^+])$ *vs.* H_2 partial pressure, at a constant CD_4 pressure of 6×10^{-6} Torr. The electron energy was 40 eV and the electron current was 0.5×10^{-8} A. Residence time in the cell, $\tau \cong 7 \times 7 \times 10^{-4}$ sec. The line of smaller dashes gives the $[H_3^+]/[H_2^+]$ ratio under the same conditions. The data were obtained from ion-ejection results similar to those of Figure 5.

incomplete resolution of the H_2^+ and H_3^+ ejection processes will be discussed shortly. A further possibility is the reaction

$$H_3^+ + CD_4 \longrightarrow CD_3H_2^+ + HD \qquad (11)$$

Such a reaction seems to imply a $CD_4H_3^+$ complex (although not necessarily), which is unlikely.

The H_2^+ ejection results in Figure 5b are not as simple to quantitatively discuss as the H_3^+ data, since ejection of H_2^+ necessarily ejects most of the H_3^+ ions also (due to reaction 1). It is clear, however, from comparison of the H_2^+ and H_3^+ ejection results, that H_2^+ undergoes the reactions

$$H_2^+ + CD_4 \begin{cases} \longrightarrow CD_4^+ + H_2 & (12a) \\ \longrightarrow CD_3^+ + H_2 + D & (12b) \\ \longrightarrow CD_2H^+ + H + D_2 & (12c) \end{cases}$$

The mechanism for the reactions 12b and 12c cannot be unambiguously specified. There may be a $[CD_4H^+]^*$ complex intermediate or the reactions may be direct.

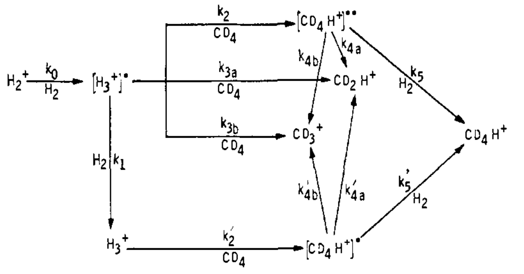

Figure 8. Reaction mechanism of H_3^+–CD_4 system necessary to explain data of Figure 7.

Reaction 12c clearly eliminates charge exchange induced decomposition of CD_4^+ as the sole source of CD_3^+. These conclusions are consistent with the results of Koopman,[18] who determined that CH_4^+ was the predominant product of charge exchange of 100-eV H_2^+ ions with CH_4. Due to resolution difficulties Koopman could not rule out the formation of small amounts of CH_3^+, however.

It should be mentioned that extreme care was taken in running the ejection experiments to work at the absolute minimum ion densities. This is essential to eliminate coulombic coupling of the equations of motion of the various ions. The experiments reported here, and in the following section, were performed with electron currents of 1×10^{-8} A or less with a resulting ion current of less than 1×10^{-11} A.

An alternate way of determining the contributions of H_2^+ and H_3^+ to the various single carbon peaks is to set the magnetic field and observing frequency at the resonance values of a given ion and then sweep the ejection frequency. Spectra of this sort are displayed in Figure 6. The contributions to the various single carbon peaks are precisely as expected from the more conventional magnetic field sweep spectra of Figure 5. One advantage of the frequency sweep method is that the resolution of the ejection process is immediately apparent. As can be seen from Figure 6a, the H_2^+ and H_3^+ peaks are very nearly totally resolved. Again great care was taken to minimize the ion density in the cell.

The dependence of the CH_5^+/CH_3^+ ratio as a function of H_2 pressure has been previously reported (in part)[12,13] with two differing mechanisms to explain the data. Aquilanti and Volpi[12] explain the data in the high H_2 pressure limit by assuming H_3^+ and CH_4 form an excited $[CH_5^+]^*$ complex, which can either decompose to CH_3^+ or be stabilized to CH_5^+ by collision with H_2. Leventhal and Friedman[13] have shown that at lower pressures the reaction of excited $[H_3^+]^*$ is important. We find the complete mechanism to contain both features. In Figure 7 the ratio $CD_4H^+/\Sigma[C(H,D)_3^+]$ is plotted as a function of H_2 pressure with a constant CD_4 pressure of 7×10^{-6} Torr. The data of Figure 7 were taken using H_3^+ ion-ejection techniques similar to Figure 5c. Figure 8 gives the complete mechanism of reaction necessary to explain the details of the pressure dependence of Figure 7.[19] At the lowest H_2 pres-

---

and L. Friedman, *J. Chem. Phys.*, **48**, 1559 (1968). If $[H_3^+]^*$ is linear and has at least 2.4-eV internal energy, then possibly the charge exchange could result at thermal energies. The expected equilibrium structure of H_3^+ is triangular, however, at least in the ground state: H. Conroy, *ibid.*, **41**, 1341 (1964).

(18) D. Koopman, *Phys. Rev.*, **178**, 161 (1969).

(19) The mechanism in Figure 8 is not necessarily unique. One possible variation would be the formation of a certain amount of H_3^+ directly from H_2^+ rather than exclusively from deactivation of $[H_3^+]^*$. There is no experimental evidence to date that bears on the relative amounts of H_3^+ and $[H_3^+]^*$ formed from H_2^+. Since there is definite evidence for formation of $[H_3^+]^*$ (ref 13 and 15) and no evidence for the

sure, the reactions of $[H_3^+]^*$ with CD_4 will dominate. This yields a value of the ratio of the rates of formation of CD_4H^+ and $C(H,D)_3^+$

$$R_0 = \left.\frac{R(CD_4H^+)_T}{R[\Sigma C(H,D)_3^+]}\right|_{H_2 \to 0} = \frac{[H_3^+]^*[CD_4]k_2 - [CD_4H^+]^{**}(k_{4a} + k_{4b})}{[H_3^+]^*[CD_4](k_{3a} + k_{3b}) + [CD_4H^+]^{**}(k_{4a} + k_{4b})} \qquad \text{(I)}$$

where

$$R(CD_4H^+)_T = R(CD_4H^+) + R([CD_4H^+]^{**})$$

If the last terms in eq I can be ignored relative to the first

$$R_0 \cong \frac{k_2}{k_{3a} + k_{3b}} \qquad \text{(II)}$$

This assumption is equivalent to assuming the $[CD_4H^+]^*$ decomposition rate constants, k_{4a} and k_{4b}, are small relative to $k_2[CD_4]$ and $(k_{3a} + k_{3b})[CD_4]$. The validity of this assumption is borne out by the relatively long lifetime of $[CD_4H^+]^*$ determined shortly. It is important to point out that it is essential to include the direct reactions k_{3a} and k_{3b} to predict an intercept other than zero at $[H_2] = 0$.[20] Aquilanti and Volpi[12] extrapolated their CH_5^+/CH_3^+ ratio data to zero at zero H_2 pressures. However, they did not report data for CH_5^+/CH_3^+ ratios of less than unity. If we ignore the two points in our Figure 7 at lowest pressure, a zero intercept would also be predicted. Leventhal and Friedman[13] report a nonzero intercept of CH_5^+/CH_3^+ for the reaction of $[H_3^+]^*$ with CH_4, in spite of the fact their $[H_3^+]^*$ ions had 3.5-eV translational energy. The reason for the curvature at lowest pressure must be due to the direct reaction of $[H_3^+]^*$ to form CD_3^+ and CD_2H^+.

At moderate H_2 pressures (1–3 × 10^{-4} Torr), and again assuming terms like $[CD_4H^+]^{**}(k_{4a} + k_{4b})$ are small, the ratio becomes

$$R_m = \frac{R_T'(CD_4H^+)}{R[\Sigma C(H,D)_3^+]} \cong \frac{[H_3^+]}{[H_2^+]}\frac{k_2'k_1}{k_0(k_{3a} + k_{3b})} + \frac{k_2}{k_{3a} + k_{3b}} \qquad \text{(III)}$$

where

$$R_T'(CD_4H^+) = R(CD_4H^+) + R([CD_4H^+]^{**}) + R([CD_4H^+]^*)$$

and it was assumed that $[H_3^+]^*$ was in a steady state. The predicted ratio is proportional to the sum of a constant times $[H_3^+]/[H_2^+]$ and R_0. From the data of Figure 2, the $[H_3^+]/[H_2^+]$ ratio is calculated and plotted as the line of smaller dashes in Figure 7. If R_0 is added to this dashed line, the curvature below 3 × 10^{-4} Torr closely resembles the experimental and supports the assumed mechanism.

Finally, at highest H_2 pressure, all of the $[H_3^+]^*$ has been moderated to H_3^+ and the ratio of the rates becomes

$$R_\infty = \frac{R(CD_4H^+)}{R(\Sigma[C(H,D)_3^+])} = [H_2]\frac{k_5'}{k_4'} \qquad \text{(IV)}$$

The predicted linear dependence of the ratio is as observed for H_2 pressures greater than 3 × 10^{-4} Torr.

From eq II, III, and IV, and Figure 7, several relative rates can be determined. These rates are collected in Table I. The value of $k_2/(k_{3a} + k_{3b})$ was taken from the intercept of Figure 7. $k_5'/(k_{4a}' + k_{4b}')$ can be calculated from the straight line at high H_2 pressures. It is straightforward to calculate the total collision rate constant of CD_4H^+ with H_2 from the theory of Gioumousis and Stevenson,[21] yielding $k_5' \cong 1.6 \times 10^{-9}$ cc molecule^{-1} sec^{-1}. From the relative rate data in Table I, $(k_{4a}' + k_{4b}') \cong 5.5 \times 10^3$ sec^{-1} or $[CD_4H^+]^*$ has a lifetime of 1.8×10^{-4} sec. This result is about two orders of magnitude larger than the lifetime of $[CH_5^+]^*$ determined by Aquilanti and Volpi.[12] The lifetime difference has little to do with a deuterium isotope effect as similar results were obtained in CH_4–H_2 mixtures.

Table I. Relative Rate Constants in Various Hydrogen–Methane Mixtures

Reaction	Relative rate
$[H_2^+]^* + CD_4 \begin{cases} \xrightarrow{k_2} CD_4H^+ \\ \xrightarrow{k_{3a}} CD_3^+ \\ \xrightarrow{k_{3b}} CD_2H^+ \end{cases}$	$k_2/(k_{3a} + k_{3b}) = 0.8$ $k_{3a}/k_{3b} = 1.0$
$\underbrace{H_3^+ + CD_4} \big\downarrow k_2' \; (CD_4H^+)^* \begin{cases} \xrightarrow{k_5'[H_2]} CD_4H^+ \\ \xrightarrow{k_{4a}'} CD_3^+ \\ \xrightarrow{k_{4b}'} CD_2H^+ \end{cases}$	$k_5'/(k_{4a}' + k_{4b}') = 2.9 \times 10^{-13}$ [a]
See Figure 8	$\dfrac{k_2'k_1}{k_0(k_{3a} + k_{3b})} \cong 1.0$
See Figure 8	$k_2'/k_2 = 1.1$
$[D_3^+]^* + CH_4 \begin{cases} \xrightarrow{k_{13b}} CH_3^+ \\ \xrightarrow{k_{13c}} CH_2D^+ \end{cases}$	$k_{13b}/k_{13c} \cong 0.5$
$[H_3^+]^* + CH_3D \begin{cases} \xrightarrow{k_{14b}} CH_3^+ \\ \xrightarrow{k_{14c}} CH_2D^+ \end{cases}$	$k_{14b}/k_{14c} \cong 0.6$

[a] Units, cc/molecule.

It should be noted that the lifetime derived here assumes a single collision deactivates $[CD_4H^+]^*$. This need not necessarily be the case, but certainly not more than a few collisions are necessary.[22] In any case, the same single collision assumption was made by Aquilanti and Volpi. The longer lifetime found in our work most likely reflects the difference in energy between the icr experiments (thermal) and the data of Aquilanti and Volpi (ion exit energies greater than 5 eV).

From the close proximity of the experimental curve $[CD_4H^+]/\Sigma C(H,D)_3^+$ *vs.* H_2 pressure to the sum of

---

formation of H_3^+ directly from H_2^+, we have chosen to exclude the direct formation of H_3^+. Inclusion of direct formation of H_3^+ does not change the qualitative conclusions of the results, but certain of the quantitative conclusions would have to be modified.

[20] Actually, the same conclusions can be obtained by postulating a superexcited intermediate that can either internally rearrange to give $[CD_4H^+]^{**}$ or decompose to give CD_3^+ or CD_2H^+. It is in this sense that the reactions to form CD_3^+ and CD_2H^+ from $[H_3^+]^*$ are called direct.

[21] G. Gioumousis and D. P. Stevenson, *J. Chem. Phys.*, **29**, 294 (1958).

[22] A typical collision rate constant between CD_4H^+ and H_2 is 2 × 10^{-9} cc molecule^{-1} sec^{-1}. Hence, for a drift time of 3 × 10^{-4} sec at 3 × 10^{-4} Torr a typical CD_4H^+ ion would undergo approximately six collisions with H_2 molecules. If the stabilization procedure is a ladder mechanism, a linear variation at high H_2 pressures would not be expected. Hence, $[CD_4H^+]^*$ is stabilized in one jump but it may take several collisions, on the average, for it to make that jump.

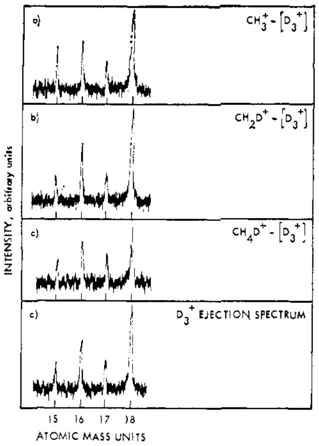

Figure 9. Pulsed-ion-ejection double resonance spectra in a mixture of 7×10^{-6} Torr CH_4 and 2.4×10^{-4} Torr D_2, 40-eV electron energy, and 1×10^{-8} A electron current. In a, b, and c, D_3^+ was continuously irradiated at 3 V/meter while being pulse-ejected from the cell; (a) CH_3^+–[D_3^+], (b) CH_2D^+–[D_3^+], (c) CH_4D^+–[D_3^+], and (d) simple D_3^+ ejection spectrum.

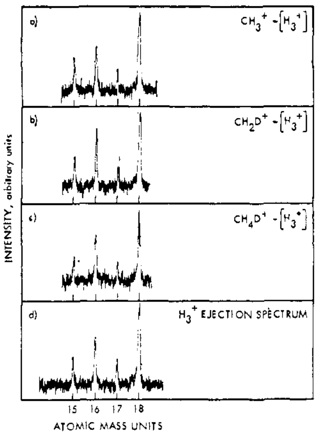

Figure 10. Pulsed-ion-ejection double resonance spectra in a mixture of 7×10^{-6} Torr CH_3D and 2.4×10^{-4} Torr H_2, 40-eV electron energy, and 1×10^{-8} A electron current. In a, b, and c, H_3^+ was continuously irradiated at 30 V/m while being pulse-ejected from the cell; (a) CH_3^+–[H_3^+], (b) CH_2D^+–[H_3^+], (c) CH_4D^+–[H_3^+], and (d) simple H_3^+ ejection spectrum.

$[H_3^+]/[H_2^+]$ and R_0 in Figure 7, it is concluded that $k_2{}^1k^1/k_0(k_{3a} + k_{3b}) \cong 1$. $k_0 = 2.11 \times 10^{-9}$ cc molecule^{-1} sec^{-1} from previous work[6] and from Gioumousis and Stevenson's theory,[21] $k_1 = 2.4 \times 10^{-9}$ cc molecule^{-1} sec^{-1}. Since Leventhal and Friedman[13] have shown that one collision is sufficient to stabilize $[H_3^+]^*$, it is not unreasonable to use the calculated value of k_1. The net result is $k_2'/(k_{3a} + k_{3b}) = 0.87$. From R_0 we can then calculate $k_2'/k_2 = 1.1$. From this analysis it appears that H_3^+ and $[H_3^+]^*$ both form CD_4H^+ at approximately the same rate.

From Figure 5c, it is evident that $[CD_3^+]/[CD_2H^+] \cong 1$ which, within the approximation of eq II, implies $k_{3a}/k_{3b} \cong 1$. Complete randomization of a CD_4H^+ complex gives $[CD_3^+]/[CD_2H^+] = {}^2/_3$. The results are sufficiently close, without consideration of an isotope effect (which would tend to equalize the ratios), to conclude that an intermediate complex mechanism is dominant at the pressures of Figure 5c. A small amount of direct reaction undoubtedly takes place, however.

In order to shed further light on the matter, the reactions

$$[D_3^+]^* + CH_4 \longrightarrow CH_4D^+ + D_2 \qquad (13a)$$

$$\longrightarrow CH_3^+ + D_2 + HD \qquad (13b)$$

$$\longrightarrow CH_2D^+ + D_2 + H_2 \qquad (13c)$$

and

$$[H_3^+]^* + CH_3D \longrightarrow CH_4D^+ + H_2 \qquad (14a)$$

$$\longrightarrow CH_3^+ + H_2 + HD \qquad (14b)$$

$$\longrightarrow CH_2D^+ + 2H_2 \qquad (14c)$$

were studied. The ion-ejection results for reactions 13 and 14 are given in Figures 9d and 10d, respectively. From the figures, $[CH_3^+]_{13}/[CH_2D^+]_{13} \cong {}^1/_2$ and $[CH_3^+]_{14}/[CH_2D^+]_{14} \cong {}^3/_5$. The completely randomized result (assuming a CH_4D^+ complex) is ${}^2/_3$. Again, if a deuterium isotope effect is taken into consideration, it appears a complex intermediate mechanism is dominant at thermal energies in these systems.

One additional way to probe the mechanism for the above reactions is to vary the kinetic energy of the reactant H_3^+ and D_3^+ molecules and observe any changes in the product distribution. The study of the energy dependence of complicated systems such as this can be carried out using pulsed-ion-ejection double resonance.[6] A secondary ion (*e.g.*, CH_2D^+) of mass m_s will have a characteristic cyclotron frequency, at magnetic field H, of $\omega_s = qH/m_sc$. At the same magnetic field, a primary ion (*e.g.*, D_3^+) of mass m_p will have a resonance frequency of $\omega_p = qH/m_pc$. If the observing oscillator is set at ω_s and an irradiating oscillator set at ω_p and the magnetic field swept, the secondary and primary ions will come into resonance simultaneously. If $\mathcal{E}_p$, the primary ion irradiating field strength at ω_p, is varied, an intensity change will be observed for the secondary ion at ω_s if the connecting chemical reaction is energy dependent. If the primary ion is pulse ejected, the variation of the secondary ion with primary ion energy can be studied in the presence of concurrent reactions forming the same secondary ion.

The results of the pulsed-ion-ejection double resonance experiments for reactions 13 and 14 are given in Figures 9a, b, and c, and 10a, b, and c. Several things are immediately obvious: (1) the CH_4D^+ intensity decreases with H_3^+ or D_3^+ kinetic energy, (2) the CH_3^+ and CH_2D^+ intensities increase with H_3^+ or D_3^+ kinetic energy, and (3) the relative magnitudes of the CH_3^+ and CH_2D^+ increases depend upon whether H_3^+ or D_3^+ is the reactant ion. Parts 1 and 2 are consistent with the standard double resonance results and will be discussed shortly. Part 3 will be considered further here. There is definite evidence that the ratio of CH_3^+/CH_2D^+ is dependent upon the translational energy of the H_3^+ or D_3^+ reactant. Further, it is interesting that the ratio decreases when H_3^+ is irradiated (from 0.6 to 0.5) and increases when D_3^+ is irradiated (from 0.5 to 0.75). The system thus appears to have a memory regarding the origin of the protons or deuterons in the CH_3^+ and CH_2D^+ product ions. This result tends to substantiate the postulate that, in part, a direct mechanism is at play in the formation of CH_3^+ and CH_2D^+, as the random decomposition of a $[CH_4D^+]^*$ complex should be independent of the reactants forming the complex. There are two possible explanations for this result. First, both hydride ion abstraction[23] and some

Table II. Double Resonance Results for Methane–Hydrogen Mixtures

System	Observed		Irradiated	Neutral[a] products	Response[b]
	amu	species			
CD_4–H_2[c]	20	CD_4^+	H_2^+	H_2	+
CD_4–H_2[c]	18	CD_3^+	H_2^+	HD + H	+
CD_4–H_2[c]	17	CD_2H^+	H_2^+	D_2 + H	+
CD_4–H_2[d]	21	CD_4H^+	H_3^+	H_2	−
CD_4–H_2[d]	20	CD_4^+	H_3^+		+
CD_4–H_2[d]	19	H_3O^+[f] (CD_3H^+)	H_3^+		−
CD_4–H_2[d]	18	CD_3^+	H_3^+	H_2 + HD	+
CD_4–H_2[d]	17	CD_2H^+	H_3^+	H_2 + D_2	+
CD_4–H_2[d]	16	CDH_2^+	H_3^+		+
CD_4–H_2[d]	15	CH_3^+	H_3^+		+
CD_4–H_2[d]	15	CH_3^+	CH_2D^+	HD	+
CH_3D–D_2[e]	19	$CH_3D_2^+$	D_3^+	D_2	−
CH_3D–D_2[e]	20	H_2DO^+[f] ($CH_2D_3^+$)	D_3^+		−

[a] Assumed in all cases the neutral reactant is CD_4 or CH_3D except when CH_2D^+ is irradiated where H_2 is the neutral reactant. [b] A positive response indicates more product ion is formed when the reactant is irradiated and a minus sign indicates less. [c] 8×10^{-6} Torr CD_4 and 8×10^{-6} Torr H_2. [d] 8×10^{-6} Torr CD_4 and 4.5×10^{-4} Torr H_2. [e] 8×10^{-8} Torr CD_4 and 4×10^{-4} Torr D_2. [f] Most likely product is H_3O^+ or H_2DO^+.

form of displacement reaction may be simultaneously operative. Hydride ion abstraction is supported by the fact that the greatest product intensity increase with energy is observed for loss of H^- from CH_4 and CH_3D. An increase is also clearly observed, however, for CH_2D^+ when D_3^+ is irradiated and impacted on CH_4 (Figure 9b), which suggests the displacement reaction. Second, for translationally hot H_3^+ or D_3^+ reactant ions the $[CH_4D^+]^*$ complex will have more internal energy and hence decompose to CH_3^+ and CH_2D^+ faster than for thermal H_3^+ or D_3^+ reactant ions. This possibility would explain the absolute increase in CH_3^+ and CH_2D^+ intensity with H_3^+ energy. The change in the CH_3^+/CH_2D^+ ratio, depending on whether H_3^+ or D_3^+ is the reactant ion, could be due to an increase in hydride ion abstraction at the expense of complex formation for the translationally hot H_3^+ or D_3^+ ions. Thus, it would not be necessary to postulate a direct displacement reaction. Regardless of the detailed mechanism, the pulsed-ion-ejection double resonances results give supporting evidence for the existence of a direct reaction to form methyl ions by impact of energetic H_3^+ ions on methane.

The response at mass 17 in Figures 9 and 10 is not well understood, but could result from the formation of CH_2D^+ followed by an exchange reaction with D_2. There was essentially no energy dependence of the mass 17 peak.

C. Double Resonance Studies. The principles of ion cyclotron double resonance have been amply described before[2–8] and will not be repeated here. It is sufficient to recall that when a particular reactant ion is translationally heated, a change in intensity of chemically connected product ions will occur if the connecting rate constant is energy dependent. The results of several double resonance studies in H_2–CD_4 and D_2–CH_3D mixtures are summarized in Table II.

From the pressure dependence results we know that the exchange reactions 4–6 occur at thermal energies. From Table II, the positive response for CH_3^+–$[CH_2D^+]$[24] can thus be interpreted as meaning the exchange rate constant increases with CH_2D^+ energy.[4b] The exchange reactions are further confirmed by the positive double resonance results of $CD_3^+ \rightarrow CH_3^+$ when H_3^+ is irradiated. Obviously only CD_3^+ and CD_2H^+ can be direct products of H_3^+ reacting with CD_4 (excluding a $CD_4H_3^+$ complex), and the positive responses for CDH_2^+ and CH_3^+ reflect a transformation of information through the 4–6 chain.

The negative response for CD_4H^+–$[H_3^+]$ (and $CH_3D_2^+$–$[D_3^+]$) unambiguously proves that reaction 3 proceeds at thermal energies. The corresponding positive responses for CD_3^+–$[H_3^+]$ and CD_2H^+–$[H_3^+]$ indicate that the production of CD_3^+ and CD_2H^+ is enhanced when the reactant H_3^+ energy is increased.[25] Leventhal and Friedman[13] obtained low values for the CH_5^+/CH_3^+ ratio (relative to our work and that of Aquilanti and Volpi[12]) when they used H_3^+ ions with 3.5-eV translational energy, which is consistent with our double resonance findings.

It is of interest to determine whether the decrease in CH_5^+ intensity with H_3^+ ion energy is compensated for by a corresponding quantitative increase in CH_3^+ intensity. The results of such an experiment are given in Figure 11. It is apparent that CH_5^+ disappears faster than CH_3^+ is formed, by a factor of approximately 2.5, as the H_3^+ ion energy is increased.[26] If one assumes H_3^+ and CH_4 undergo "strong coupling collisions," then the phase space theory of Light[27] indicates that particular reaction probabilities will vary with reactant ion energy, but the total reaction probability will remain constant. No significant charge exchange was observed

---

(23) Hydride ion abstractions have been known for some time between alkyl ions and alkanes: F. H. Field and F. W. Lampe, *J. Amer. Chem. Soc.*, **80**, 5587 (1958).

(24) CH_3^+–$[CH_2D^+]$ implies that CH_3^+ is observed while CH_2D^+ is irradiated.

(25) At the relatively high H_2 partial pressures of the double resonance data in Table II, it is assumed that all of the $[H_3^+]^*$ is moderated to H_3^+ and that the methyl ions are formed (at thermal energies) strictly from the decomposition of a CD_4H^+ complex. It is possible both a direct reaction and decomposition of an excited CD_4H^+ complex simultaneously form $C(H, D)_3^+$ ions from translationally hot H_3^+.

(26) There are two limits in which the reactant ion energy can be calculated: (1) the zero collision-time limited case, $KE_{\text{time}} = q^2\mathcal{E}^2_{\text{rf}}\tau^2/8 \cdot m_p$, and (2) the collision limited case, $KE_{\text{collision}} = q^2\mathcal{E}^2_{\text{rf}}/(m_p + M)/8\, \xi_p^2 m_p^2$ (see ref 4–7). The experiments reported in Figure 11 were taken under conditions midway between the two extremes and hence neither is strictly applicable. However, since both give reactant ion energies proportional to the square of the irradiating field strength, $\mathcal{E}_{\text{rf}}$, the abscissa of Figure 11 is proportional to energy. The maximum energy is of the order of 2–3 eV.

(27) J. C. Light, *J. Chem. Phys.*, **40**, 3221 (1964).

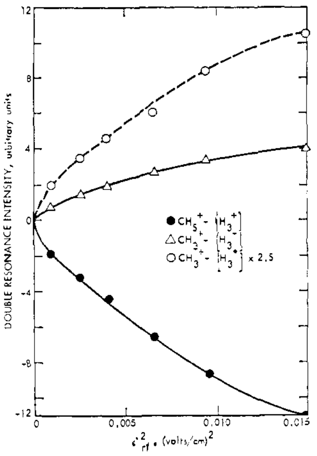

Figure 11. Dependence of the double resonance intensities of CH_5^+–$[H_3^+]$ and CH_3^+–$[H_3^+]$ as a function of the square of the irradiating field strength (see ref 26).

between H_3^+ and CH_4 over the entire energy range of Figure 11. Hence, either a significant number of nonreactive scattering collisions occur (~50%) or Light's theory is not applicable to this system. Aquilanti and Volpi[12] measured a rate constant for reactions of H_3^+ with CH_4 that was approximately 50% of the collision rate constant calculated by the Langevin theory[21] which is consistent with our double resonance results. A similar circumstance was found for H_2^+–Ar reactions,[8] while H_2^+–N_2 reactions[7,8] closely follow Light's hypothesis.

Conclusion

The ion–molecule reactions in methane–hydrogen mixtures are seen to be quite complex. A variety of condensation, atom-exchange, and charge transfer reactions take place. Perhaps the most interesting feature is the variation of the CH_5^+/CH_3^+ ratio with H_2 pressure, resulting from the reaction of H_3^+ with CH_4. In order to explain the details of the pressure dependence it is necessary to postulate distinct reactions of both excited $[H_3^+]^*$ and collisionally deactivated H_3^+. $[H_3^+]^*$ reacting with CH_4 forms CH_3^+ primarily *via* a direct mechanism, while H_3^+ first forms $[CH_5^+]^*$, which can be subsequently stabilized or decomposed to CH_3^+ and H_2. The lower limit of the lifetime of the $[CD_4H^+]^*$ ion was estimated to be approximately 2×10^{-4} sec.

Significant isotopic exchange occurs between $C(H,D)_3^+$ and $(H,D)_2$. The resulting isotopically mixed methyl ions can further react with methane to give isotopically mixed $C_2(H,D)_5^+$ ions, as noted by Inoue and Wexler.[28]

Acknowledgment. The authors gratefully acknowledge support of the Directors' Discretionary Fund of the Jet Propulsion Laboratory, California Institute of Technology, Pasadena, California.

(28) M. Inoue and S. Wexler, Abstracts of the 157th National Meeting of the American Chemical Society, Minneapolis, Minn., April 1969, No. Phys 054.